

International Journal of Pharmacy and Biological Sciences ISSN: 2321-3272 (Print), ISSN: 2230-7605 (Online)

IJPBS™ | Volume 8 | Issue 3 | JUL-SEPT | 2018 | 1177-1184



Research Article | Biological Sciences | Open Access | MCI Approved

MOLECULAR MODELLING AND DOCKING STUDIES OF NATURAL COMPOUNDS AGAINST PACHYTENE CHECKPOINT PROTEIN 2 HOMOLOG

Sahaja Thippani, Kamala Dorathy Priya S, Rumana Waseem, Seshagiri Bandi^{*}, Mahmood Shaik Bioinformatics Wing, Mycology & Plant Pathology Lab, Department of Botany, University College of Science, Osmania University, Hyderabad-500007

*Corresponding Author Email: giri.bandi@gmail.com

ABSTRACT

The present study explains computational methods to design thermostable "Pachytene checkpoint protein 2 homolog" of Homo sapiens proteins using the sequence available from uniprot (UniProtKB – Q15645). Homology modelling study was performed to generate a 3D model of Cytochrome b protein. The model was developed by using Modeler9.19 software tool. The developed model was further docked with natural compounds such as Aaptosamine, Aaptosine, Aaptamine, Sesbanimide C using the AUTODOCK4.2 software tool. After designing the model molecular docking studies were performed by using Autodock4.2 with natural compounds to identify the functional effect of protein. The developed model shows above 90% of the amino acids in most favored region. The docking investigation of modelled "Pachytene checkpoint protein 2 homolog" with natural flavonoids Chrysin, Diosmetin, Galangin, Nobiletin, Puerarin and Silibinin using Autodock4.2 software. Six natural flavonoids were docked against "Pachytene checkpoint protein 2 homolog" protein. All the ligands show good binding energy and interactions. These studies provide understanding and interpreting the data produced by these methods. It explains to understand molecular interactions at the active site region.

KEY WORDS

Homology modeling, "Pachytene checkpoint protein 2 homolog", Natural flavonoids, Molecular Docking

INTRODUCTION

Thyroid hormone receptor interacting protein 13 (TRIP13) is an evolutionarily conserved protein sharing sequence homology with many other proteins ranging from yeast to humans^{1,2}. It belong to the family of AAA-ATPases, special group of ATP dependent proteases that facilitate assembly or degradation of protein complexes that regulate diverse cellular processes^{3,4}. TRIP13 has been found to be associated with regulation of spindle assembly checkpoint, chromosome synapsis and meiotic recombination hence playing an important role in DNA structural dynamics at the genomic level⁵. Moreover, it is one of the genes related to chromosomal instability⁶ and is also linked to DNA repair mechanisms in somatic cells⁷.

It was shown to be positively connected with the progression of many cancers. Transcription profiling experiments identified TRIP13 as one of the multiple cancer 'signatures' that are overexpressed in breast cancer samples⁸, the same has been confirmed by The Cancer Genome Atlas project⁹. Recent evidences has shown that is overexpressed in colorectal cancer and thus may serve as potential biomarker and therapeutic target for colorectal cancer^{10,11}. Overexpression of TRIP13 was also reported in lung adenocarcinoma, multiple myeloma and chronic lymphocytic leukemia 12, ^{13, 14}. In neck and head cancer, TRIP13 plays a critical role in DNA repair by triggering DNA protein kinase (DNA-PK) through non-homologous end joining (NHEJ) pathway. It also promotes early stages of double-strand DNA break (DSB) repair during meiotic recombination and



following exposure to radiation and chemotherapy. Its ability to repair damaged DNA through the activation of DNA repair pathways induces treatment-resistance in head and neck cancers promoting tumor progression ¹⁵, Pressly et al demonstrated that TRIP13 can act as a compensatory stress-response protein in response to acute renal tubular injury in humans. TRIP13 repair damaged tubular epithelial cells following ischemia-reperfusion injury (IRI), a renal stress condition central to the pathogenesis of acute kidney injury (AKI). By its ability to reverse the cellular damage by regulating DNA repair pathways, TRIP13 can be used as a viable therapeutic target to treat AKI ¹⁷.

These findings suggest the importance of TRIP13 in cell division and DNA repair mechanisms and its ability to function as a key surveillance protein to help assess DNA integrity.

In the present study, an effort was made to generate the 3-Dimensional structure of the Pachytene checkpoint protein 2 homolog protein sequence (Uniprot accession number: Q15645) from Homo sapiens. Modeller9.19 was used for the homology modelling. The model was validated by using PROCHECK. Present study could provide useful information to get the functional characterization of this protein.

METHODOLOGY:

Homology modelling

The amino acid sequence of Pachytene checkpoint protein 2 homolog was retrieved from Uniprot ¹⁸. A three-dimensional model was generated for "Pachytene checkpoint protein 2 homolog". A sequence similarity search was performed to identify the structural similarity of the query sequence by using Protein BLAST ¹⁹ tool by selecting database against Protein Data Bank (PDB) for identifying template for homology model building ²⁰. The template protein (PDB ID: 4XGU) was identified on the basis of E-value (lesser the E-value higher the similarity), >30% identity, maximum score. Comparative sequence alignment studies were performed with query and template structure using ClustalX tool and online ClustalW tools ²¹.

MODELLER9.19 software was used to develop the model. It is an automated approach to comparative modeling by satisfaction of spatial restrains 22. To align the query and template sequences manually the input file of alignment. Ali was used in MODELLER 9.19. After completion of alignment twenty models were generated and all the generated models were thermodynamically minimized using molecular dynamics and simulation approach. By implementing MODELLER9.19²³ auto-model class, calculated 3D models of the target automatically. The best model which is having smallest value was selected on the basis of Lowest Objective Function. Generate model was then checked in detail for protein structure stereochemistry including Ramachandran plot and Psi/Phi angles using PROCHECK 24.

Molecular docking studies

All the natural flavonoid molecules were collected from scientific literature and sketched in SYBYL6.7 ²⁵ and energetically minimized by adding. The molecules were then saved in.mol 2 formats for molecular docking purpose. Molecules used in the present study are shown in table 1.

Molecular docking studies were performed to explain the binding mode of proteins and alkaloid complexes. All the plant derived complex molecules were docked by using Autodock 4.2 software ²⁶. All the molecules were docked individually in Autodock4.2. The modelled three-dimensional structure of Pachytene checkpoint protein 2 homolog protein was imported to Autodock4.2 and structurally optimized by adding hydrogens to protein allocated with kollaman charges. After adding the hydrogens, the model was saved in PDBQT format, later ligands were prepared by optimizing the torsion angles and saved them in PDBQT format. Potential binding site for the Pachytene checkpoint protein 2 homolog modelled protein was identified using SYBYL6.7. A grid was generated around to identify xyz coordinates around binding site of Pachytene checkpoint protein 2 homolog protein. Lamarckian genetic algorithm (LGA) was selected for freezing, docking and default parameters used in autodock4.2.



Table 1: Structures of flavonoids used in the present study

RESULTS AND DISCUSSION

After sequence alignment and homology modeling of Pachytene checkpoint protein 2 homolog shows highly conserved regions in amino acid sequences are shown in Figure 1. The most homologous template for building a homology model for checkpoint protein 2 was identified through protein blast algorithm. Based upon the homology search, Crystallographic structure of Chain A, Structure of C. Elegans Pch-2 (PDB ID: 4XGU) was selected as a template. Twenty models were generated using Modeler 9.19 program. The alignment file was tweaked manually to excellent fit in the sequences. After the generated models for all the primary sequences, the model with least object function was selected for further protein stereochemistry evaluation (phi and psi angles) with Procheck software. The three $(\emptyset, \Psi \text{ and } \omega)$ backbone torsion angles are important determinants of a protein fold. PROCHECK software generates a number of scatter plots, these are known as Ramachandran plots. These plots show complete residue by residue data and the assessment of the generally excellence of the producing structure as

compared to well refined structures of the same The Ramachandran plot is the main resolution. indicator to check the intrinsic quality of the protein structure. The Ramachandran plot of the 4XGU shows 325 amino acid residues (95.3%) in most favorable regions with 16 amino acid residues (4.7%) falling into additionally allowed regions, and there is no amino acid residue in the generously allowed region and disallowed region, whereas for the modeled protein shows, 363 amino acid residues (90.8%) in the most favorable region, 32 amino acid residues present in additionally allowed region (8.0%) and 5 amino acid residues in generously allowed region (1.3%). There is no amino acid residue present in disallowed region. These results clearly indicate that the generated protein model is more conformationally superior to the template structure. Figure 2 and 3 represents cartoon model of TRIP13 protein and Ramachandran plot respectively. The modeled structure was superimposed with the template 4XGU by using SPDBV, it was observed that RMSD value on superposition of the modeled structure of checkpoint protein 2 with the template structure was also calculated.



```
CLUSTAL O(1.2.4) multiple sequence alignment
sp|Q15645|PCH2_HUMAN odb|4XGU|A PachyteneCheckpointProteinMHEPMKTLKNIHAEIRIC-----QKF-PKSTVQ 53

    sp|Q15645|PCH2_HUMAN
    EAVGDLKQALPCVAESPTVHVEVHQRGSSTAKKEDINLSVRKLLNRHNIVFGDYTWTEFD
    111

    pdb|4XGU|A
    KRFSEFEELIKAASK------NA-----RNWKPISSVELFQGDSSLNELF
    92

                           1 ...... 1 .....
pdb | 4XGU | A
                           EKLV---IGTCELRDGELF---ENVNDLTINPSNIHVYKLHKDGPLSQNIGDDDGDESII 146
                            * :: : : * ** : **:
                                                                 :*:::*::*** *:*: ::

    sp|Q15645|PCH2_HUMAN
    AANHWVLPAAEFHGLWDSLVYDVEVKSHLLDYVMTTLLFSDKNVNSNLITWNRVVLLHGP
    229

    pdb|4XGU|A
    GSQLWQLPCVEFDSIWENLIYDSNLKNEVMSYVAALARLSEKHVNTKIINVNRLILLTGP
    206

                           .:: * **..**..:*: ** ::*..:: .** :
                                                                     ******** *** ***
sp|Q15645|PCH2_HUMAN
                        PGTGKTSLCKALAQKLTIRLSSRYRYGQLIEINONSLFSKWFSESGKLVQKMFDQIDELA 266
                            PGTGKTSLCKALAQKLTIRLSSRYRYGQLIEINSHSLFSKWFSESGKLVTKMFQKIQDLI 289
pdb | 4XGU | A
                                                        *************
sp|Q15645|PCH2_HUMAN DDKDALVFVLIDEVESLTAARNACRAGTEPSDAIRVVNAVLTQIDQIKRHSNVVILTTSN 349
                            EDEKCMVFVLIDEVESLGMCRESSSSRSEPSDAIRAVNALLTQIDRIRRRDNVLILCTSN
pdb|4XGU|A
                            :*:..:********
                                                 sp|Q15645|PCH2_HUMAN ITEKIDVAFVDRADIKQYIGPPSAAAIFKIYLSCLEELMKCQIIYPRQQLLTLRELEMIG 409
pdb|4XGU|A LESTLDKALVDRADIVKNVGQPSDFARYSMLKSSIMELARIGVVIDNEVHTDYWPQDIC- 385

    sp|Q15645|PCH2_HUMAN
    FIENNVSKLSLLLNDISRKSEGLSGRVLRKLPFLAHALYVQAPTVTI--EGFLQALSLAV
    467

    pdb|4XGU|A
    DTKAPRNEFTEILFKIAQEARGLSGRAISMLPTLV---YSKSPEETITLPNCMNLFLEAV
    442

                                 ....* * ***** ** * * * * **
sp|Q15645|PCH2_HUMAN
                            DKQFEERKKLAAYI
pdb|4XGU|A
                            KERLSRNN-----
                                                    450
                            .:::...:
```

Figure 1: Molecular alignment of query and template sequences

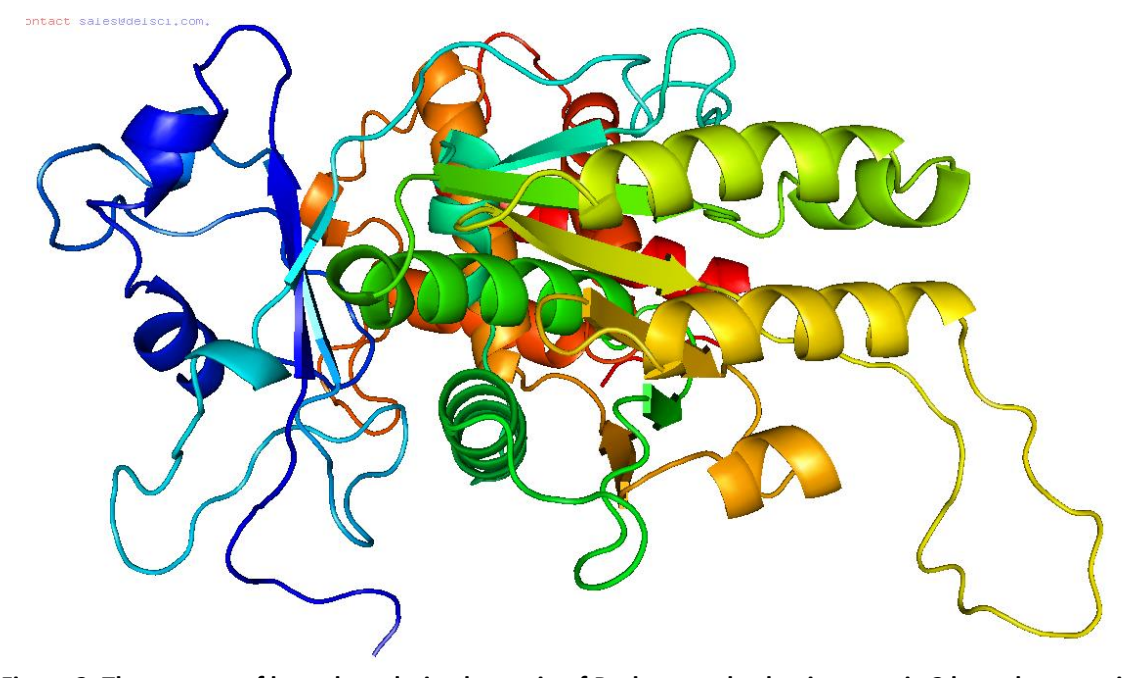


Figure 2: The cartoon of homology derived protein of Pachytene checkpoint protein 2 homolog protein



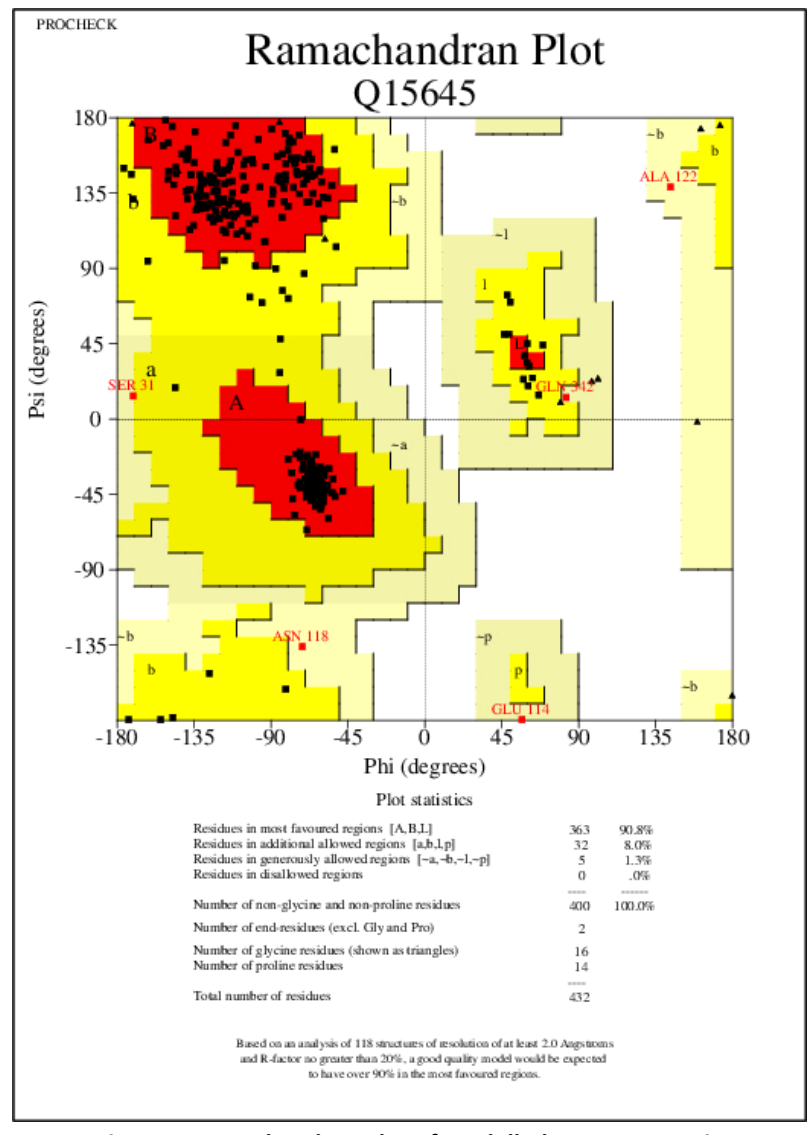


Figure 3: Ramachandran Plot of modelled TRIP 13 protein

Molecular docking Results:

Molecular docking study was performed to modeled protein by taking plant secondary metabolites into the binding site of a receptor and estimating the binding affinity of the ligand is a most important part of the structure-based drug design process. The molecular docking results indicate that all of the studied alkaloid compounds occupy an almost similar space in the binding site. Diosmetin shows best possible binding mode against modelled Albumin-1. During the molecular docking procedure, the program selects only best fit active site pocket of the protein with respect to the ligands in order to dock them. AutoDock 4.2, provides information on the binding orientation of ligands at the active site region. The docking program place both ligand and protein in different orientations,

conformational positions and the lowest energy confirmations which are energetically favorable are evaluated and analyzed for interactions. Free energies of binding (ΔGb) and dissociation constants (Ki) as calculated by AutoDock are summarized.

For all the molecules binding affinity was characterized by binding energy (ΔG) value. Ligand Diosmetin shows highest binding energy of -6.20 Kcal/mol with interacting Lys168. Nobiletin interacts with one amino acid residue Arg155, Lys168(2) with a docking score of -6.03 Kcal/mol. Chrysin shows binding energy of -5.85 Kcal/mol with interacting Lys168, Ser23 Kcal/mol score. Among 6 metabolites Diosmetin shows best binding energy and interactions. All the docking poses of the molecules were shown in table 2.



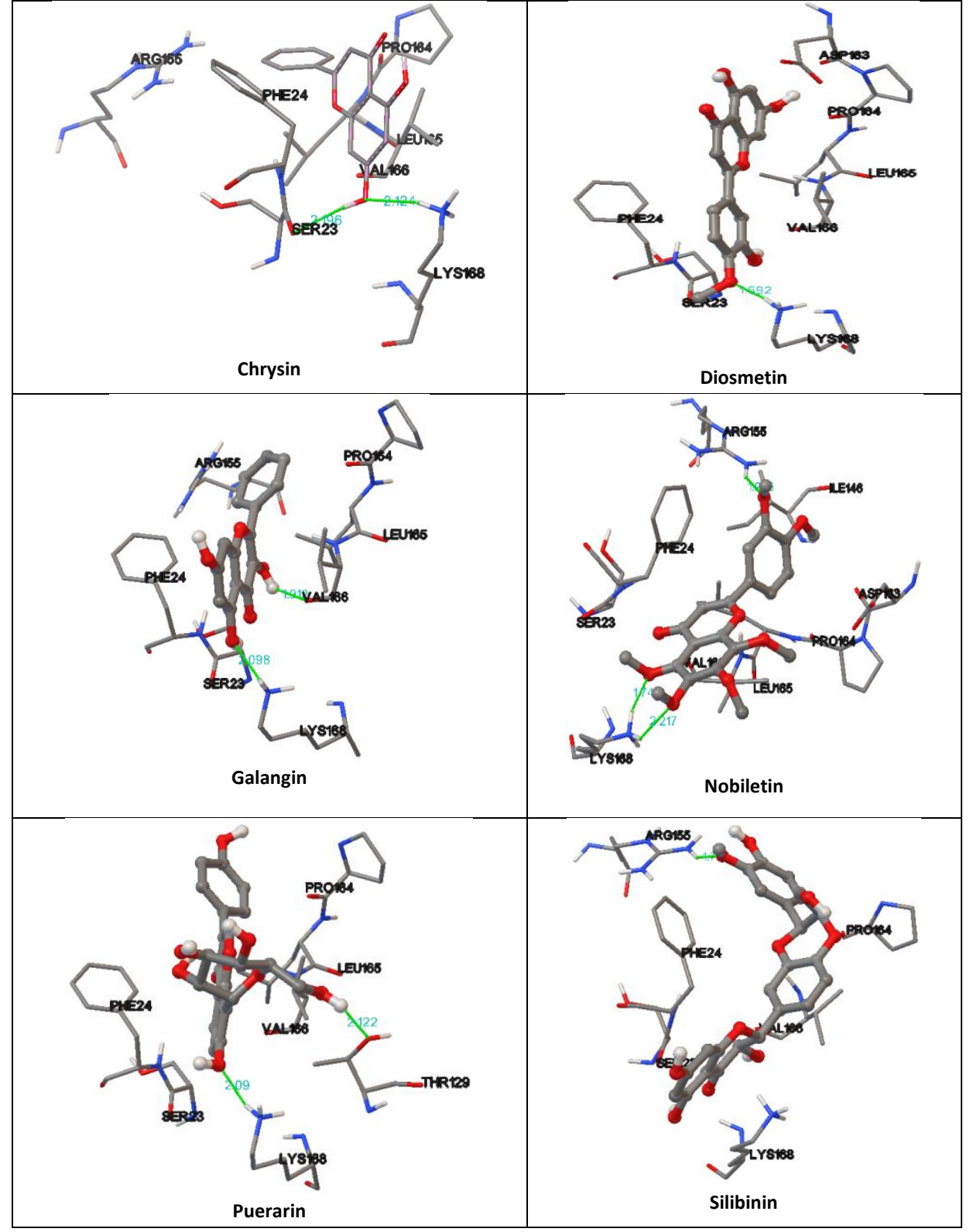


Table 2: Docking interactions of Pachytene checkpoint protein 2 homolog with natural flavonoids



CONCLUSION

In this work, homology modeling and molecular docking studies were performed to explore structural features and binding mechanism of flavonoid derivatives as Pachytene checkpoint protein 2 homolog inhibitors, and to construct a model for designing new Pachytene checkpoint protein 2 homolog protein. Homology derived model statistics are similar to template i.e., crystal structure. Docking the modelled Pachytene checkpoint protein 2 homolog protein with natural flavonoid compounds provided insight into the binding and interaction of compounds with the protein. Further, the structure-based drug discovery process along with protein information of drug targets may improve our understanding towards in-sight of mechanism of protein-ligand interactions and their binding patterns.

REFERENCES

- Lee, J. W., Choi, H. S., Gyuris, J., Brent, R. & Moore, D. D. Two classes of proteins dependent on either the presence or absence of thyroid hormone for interaction with the thyroid hormone receptor. Molecular endocrinology 9, 243–254, (1995).
- 2. Li, X. C. & Schimenti, J. C. Mouse pachytene checkpoint 2 (trip13) is required for completing meiotic recombination but not synapsis. PLoS genetics **3**, e130, (2007).
- 3. Langer, T. AAA proteases: cellular machines for degrading membrane proteins. Trends in biochemical sciences **25**, 247–251 (2000).
- Neuwald AF, Aravind L, Spouge JL, Koonin EV. AAA+: A class of chaperone-like ATPases associated with the assembly, operation, and disassembly of protein complexes. Genome Res. 9:27–43, (1999).
- 5.Vader, G. Pch2 (TRIP13): controlling cell division through regulation of HORMA domains. *Chromosoma* 124, 333–339 (2015).
- Carter S. L., Eklund A. C., Kohane I. S., Harris L. N., Szallasi Z. A signature of chromosomal instability inferred from gene expression profiles predicts clinical outcome in multiple human cancers. Nat. Genet. 38, 1043–1048, (2006).
- Banerjee, R. et al. TRIP13 enhances DNA repair to promote treatment resistance in cancer. Oral Surgery, Oral Medicine, Oral Pathology and Oral Radiology, Volume 118, Issue 6, e183, (2014).
- Rhodes D. R., Yu J., Shanker K., Deshpande N., Varambally R., Ghosh D., Barrette T., Pandey A., Chinnaiyan A. M. Large-scale meta-analysis of cancer microarray data identifies common transcriptional profiles of neoplastic transformation and

- progression. Proc. Natl. Acad. Sci. U.S.A. 101, 9309–9314, (2004).
- Cancer Genome Atlas Network Comprehensive molecular portraits of human breast tumours. Nature 490, 61–70, (2012).
- Sheng, N., Yan, L., Wu, K., You, W., Gong, J., Hu, L., Wang, Z. TRIP13 promotes tumor growth and is associated with poor prognosis in colorectal cancer. *Cell Death & Disease*, 9(3), 402, (2018).
- Kurita, K., Maeda, M., Mansour, M. A., Kokuryo, T., Uehara, K., Yokoyama, Y., Senga, T. TRIP13 is expressed in colorectal cancer and promotes cancer cell invasion. *Oncology Letters*, 12(6), 5240–5246, (2016).
- 11. Li W, Zhang G, Li X, Wang X, Li Q, Hong L, Shen Y, Zhao C, Gong X, Chen Y, Zhou J. Thyroid hormone receptor interactor 13 (TRIP13) overexpression associated with tumor progression and poor prognosis in lung adenocarcinoma. Biochem Biophys Res Commun. 499 (3):416-424, (2018).
- Tao, Y., Yang, G., Yang, H., Song, D., Hu, L., Xie, B., Shi, J. TRIP13 impairs mitotic checkpoint surveillance and is associated with poor prognosis in multiple myeloma. Oncotarget, 8(16), 26718–26731, (2017).
- Zhou, K., Zhang, W., Zhang, Q., Gui, R., Zhao, H., Chai, X., Song, Y. Loss of thyroid hormone receptor interactor 13 inhibits cell proliferation and survival in human chronic lymphocytic leukemia. Oncotarget, 8(15), 25469–25481, (2017).
- 14. Banerjee, R. et al. TRIP13 promotes error-prone nonhomologous end joining and induces chemoresistance in head and neck cancer. Nature communications. 5, 4527, (2014).
- 15. Roig, I. et al. Mouse TRIP13/PCH2 is required for recombination and normal higher-order chromosome structure during meiosis. PLoS genetics 6, (2010).
- Pressly, J. D., Hama, T., Brien, S. O., Regner, K. R., & Park,
 F. TRIP13-deficient tubular epithelial cells are susceptible to apoptosis following acute kidney injury. Scientific Reports, 7, 43196, (2017).
- UniProt Consortium T, UniProt: the universal protein knowledgebase. Nucleic Acids Res. 46(5):2699, (2018), doi: 10.1093/nar/gky092.
- Altschul, S.F., Gish, W., Miller, W., Myers, E.W. & Lipman, D.J. "Basic local alignment search tool." J. Mol. Biol. 215:403-410, (1990).
- Ye Q, Rosenberg SC, Moeller A, Speir JA, Su TY, Corbett KD1. TRIP13 is a protein-remodeling AAA+ ATPase that catalyzes MAD2 conformation switching. Elife. 4, (2015). doi: 10.7554/eLife.07367.
- Larkin MA, Blackshields G, Brown NP, Chenna R, McGettigan PA, McWilliam H, Valentin F, Wallace IM, Wilm A, Lopez R, Thompson JD, Gibson TJ, Higgins DG.

Int J Pharm Biol Sci.



- Clustal W and Clustal X version 2.0. Bioinformatics 23(2):2947–2948, (2007). doi:10.1093/bioinformatics/btm404.
- Eswar N, Webb B, Marti-Renom MA, Madhusudhan MS, Eramian D, Shen M-y, Pieper U, Sali A. Comparative protein structure modeling using modeller. In: Current protocols in bioinformatics. Wiley, New York. (2002). doi:10.1002/0471250953.bi0506s15
- Sali A, Blundell TL. Comparative protein modelling by satisfaction of spatial restraints. J Mol Biol 234(3):779– 815, (1993). doi:10.1006/jmbi.1993.1626

Received:04.05.18, Accepted: 07.06.18, Published:01.07.2018

- Laskowski RA, MacArthur MW, Moss DS, Thornton JM. PROCHECK: a program to check the stereochemical quality of protein structures. J Appl Crystallography 26(2):283–291, (1993). doi:10.1107/S0021889892009944.
- 24. SYBYL, Version 6.8 (2000) Tripos Associates, St. Louis, MO.
- Morris, G. M., Huey, R., Lindstrom, W., Sanner, M. F., Belew, R. K., Goodsell, D. S. and Olson, A. J. Autodock4 and AutoDockTools4: automated docking with selective receptor flexiblity. J. Computational Chemistry, 16: 2785-91, (2009).

Corresponding Author: Seshagiri Bandi

Email: giri.bandi@gmail.com